NUMERICAL INVESTIGATION OF C-RATE EFFECT ON TEMPERATURE VARIATION OF CYLINDRICAL 18650 LI-ION BATTERY

Pradeep Singh[1,*], Shikha Bhatt[1], Rana Manoj Morya[1]

[1]Mechanical Engineering Department

Oriental College of Technology, Patel Nagar, Bhopal, India (462022)

*Corresponding Author

Email: erpradeep3408@gmail.com

Abstract

The performance and safety of lithium-ion batteries in electric vehicles are significantly influenced by their thermal behavior during charging and discharging. This study numerically investigates the effect of C-rate on the temperature distribution of cylindrical 18650 Li-ion cells using ANSYS 2024 R1. A battery module consisting of sixteen cells was modeled under forced air cooling at an inlet velocity of 0.1 m/s. The results demonstrate that temperature rise is directly dependent on C-rate, with negligible gradients at 1C, moderate thermal hotspots at 3C, and substantial heating at 5C, particularly in centrally located cells due to reduced exposure to airflow. The findings highlight the critical role of effective battery thermal management systems (BTMS) in mitigating thermal gradients and ensuring operational safety. This work provides insights into optimizing cooling strategies to enhance battery performance and reliability in high-demand applications such as electric vehicles.

Keyword: Li-ion Battery; Numerical Analysis; EVs; C-rate; BTMS

1. Introduction

As energy demands surge in the modern world, fossil fuels remain the dominant source, accounting for roughly 80% of all energy produced. Due to their finite nature and the environmental impact of their combustion, using fossil fuels presents several drawbacks. The contribution in global greenhouse gas (GHG) emission through transportation sector is found the major contributor in 2022 accounting about 14% [1]. It was studied that GHG emission can upsurge up to 21 billion metric tons in the year 2050. As a result, there is growing global interest among researchers and entrepreneurs in developing the transportation solutions which generate less pollution. In the present time, electric vehicles (EVs) transport system is the area of interest. It works on the chemical energy of the battery, emerging as a highly viable alternative to traditional gasoline-powered vehicles [2]. The important parts of the EVs are the chassis, electric motors, battery. Battery stands out as the most vital, as it directly affects the charging and discharging rates, thereby determining the vehicle's driving range [3]. Different types of batteries like Lithium ion battery (LIB), Nickel Metal Hydride (NMH), Lead Acid battery (LAB) etc. are installed in the EVs on the basis of their operating conditions [4-6].

In recent time, Cylindrical cells have emerged as the preferred choice for electric vehicle batteries due to several compelling advantages like high energy density, high volumetric efficiency, mechanical integrity and compactness [7, 8]. A bundle of cylindrical cells is housed in a battery pack. A Battery Pack System is a unit store energy in electric vehicles (EVs), composed of interconnected lithium-ion cells arranged in modules, supported by thermal, electrical, and mechanical subsystems as shown in **Fig. 1**. It converts and stores electrical energy

for propulsion, auxiliary functions, and regenerative braking [9]. The performance, safety, cost, and range of an EV critically depend on the design and operation of its battery pack system [10].

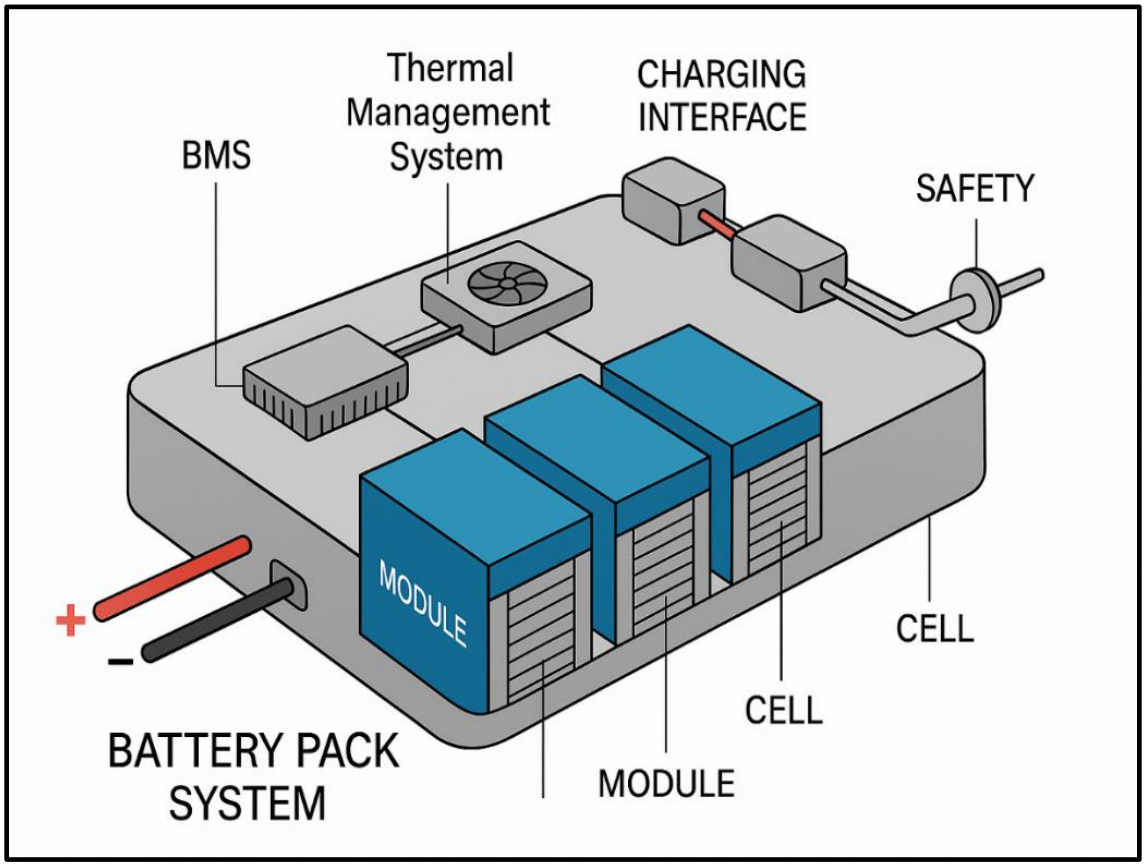

Fig. 1. *Battery pack system showing cell, module, BMS, BTM), charging interface and safety device.*

Uneven temperature difference of the cell within the battery pack cause some severe problems, ultimately resulting in a reduction of battery capacity [11]. An EV's primary goals of extended range and quick charging depend on effective battery temperature management. A primary concern with LIBs is increment in temperature during charging or discharging at high rate, which can result in adverse consequences like thermal runway, capacity reduction of the battery, and potential explosion [12]. BTMS can be done by the active or passive methods. **Fig. 2** illustrates

that external BTMSs are either active or passive. Active BTMSs work by using a circulating fluid (air, water, or other liquids) to dissipate heat rapidly which generate in the battery cell [13]. A passive BTMS manages battery heat without relying on energy-consuming systems, using techniques like PCM or heat pipes instead.

In contrast, a hybrid BTMS combines both passive and active approaches to achieve superior performance compared to using either method on its own. Depending on the specific application, BTMSs can be designed to either raise or lower the battery pack temperature as needed.

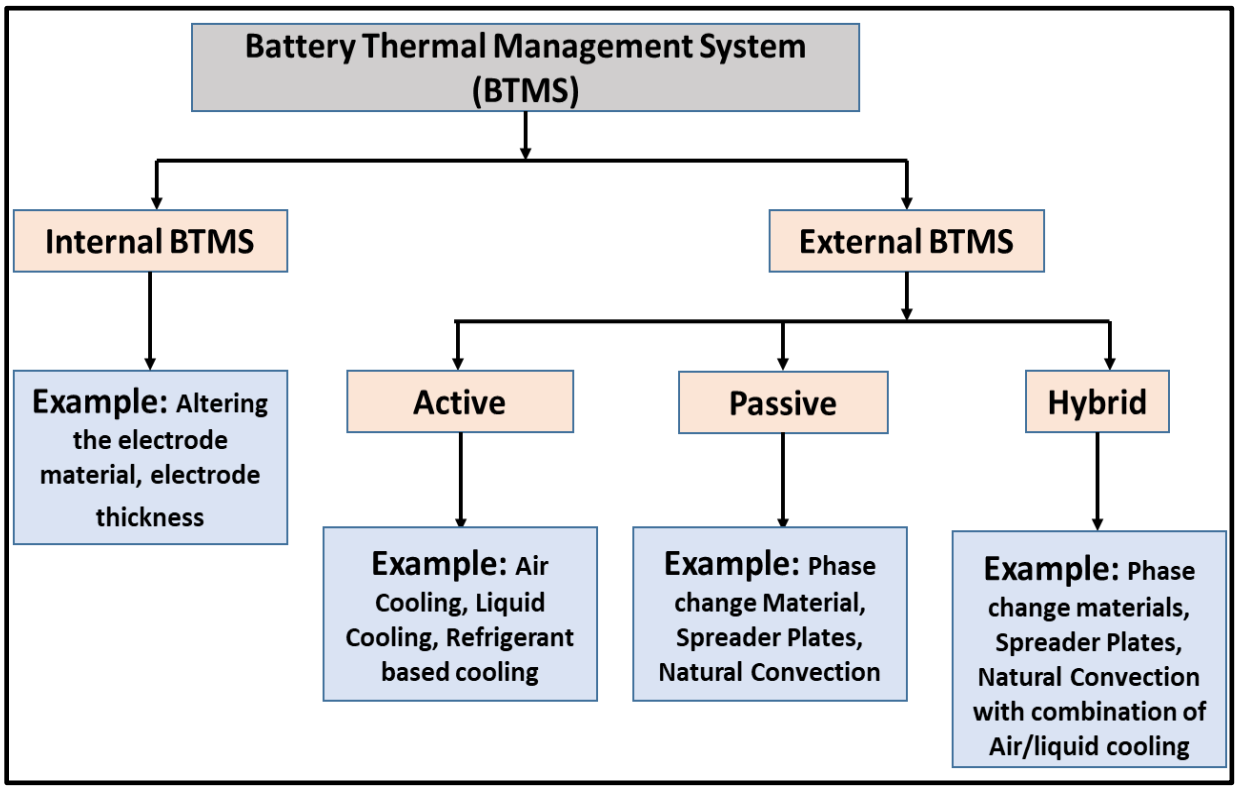

Figure 2. *Various types of BTMS*

C-rate is a simple, widely used way to express how quickly a battery is being charged or discharged relative to its rated capacity [14]. If a cell is at 1C, it will be fully charged or discharged in one hour; at 0.5C it takes two hours; at 2C it takes half an hour, and so on. Because

C-rate scales with current, it directly controls the amount of heat generated inside a battery during operation, which makes it a critical parameter for thermal management design and operation. In the present study, effect of C-rate on the cell temperature is explored with the help of numerical analysis method.

2. Materials and Method

2.1.Specification of the battery

A battery module containing cylindrical 18650 type cell is used for the analysis purpose. The specification of 18650 LIB cell is represented in **Table 1.** The electrode materials of this battery cell are LiFePO4 (anode) and graphite (cathode) [15]. The dimensional, physical and thermal specifications of the 18650 LiB cell is given in Table 3.1 [16]. It has the nominal voltage of 3.6 volt with rated capacity 3540 mAh.

Table 1. Specifications of the parameters of different properties of the 18650 battery [16]

Property	Parameter	Specification
Dimensional	Diameter	18 mm
	Height	65 mm
Physical	mass	47 g
	density	2782 kg/m^3
Electrical	Nominal Voltage	3.6 V
	Max. Voltage during charging and discharging	4.2 V and 2 V
	Standard Charge and maximum discharge current	1.675 A and 10A
	Rated Capacity	3540 mAh
	Resistance	25 Ω
Thermal	C_p	1087 J/kg.K
	Radial and axial K	1.274 and 27.584 W/m.K
	Heat generation rate (Q_g) (1C)	24277.22 W/m^3
	Q_g (2C)	68989.15 W/m^3

	Q_g (3C)	134135.79 W/m^3
	Q_g (4C)	219717.13 W/m^3

2.2. Numerical Modelling

In the present work ANSYS-2024R1software is used for the numerical analysis. The geometries are created in the Design modeller which is an integrated software of ANSYS. In geometry creation, a battery containing 16 cells of 18650 type with their specified dimensions was prepared covered by a cuboid casing having the size 9292 was prepared as shown in the Fig. 3 (a), (b), and (c). To prevent the battery from the direct contact with fluid, an aluminium envelop of thickness 0.5 mm was employed on the surface of battery (Fig. 3 (d). In the case of analysis of influence of C-rate on battery temperature, the casing is taken as hypothetical control volume in which a fluid air is passed from the specified inlet to the outlet.

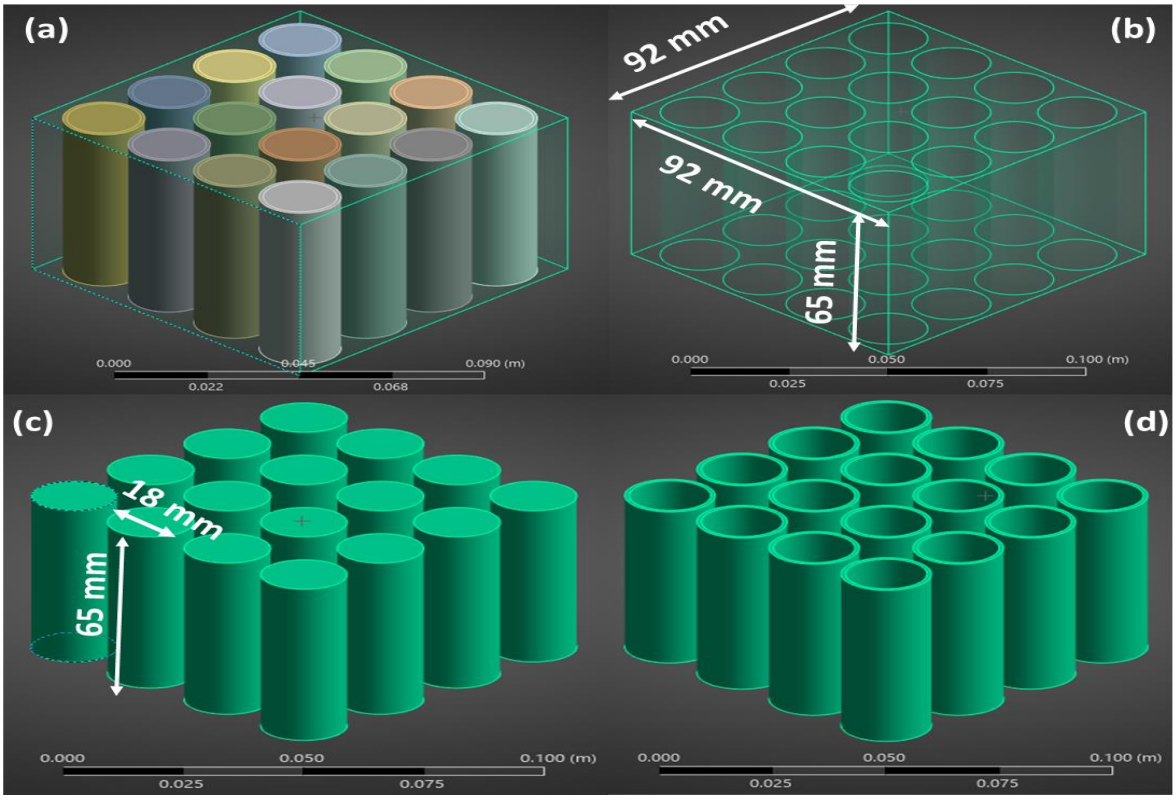

Fig. 3. Battery assembly of cell and casing; (a) Cells and casing; (b) dimensions of casing; (c) dimension of 18650 cell; (d) cell cover having thickness 0.5 mm.

Meshing is done and it is optimized for the cell with PCM case having the PCM as capric acid. During ANSYS setup, 3D precision was used with maximum 4 processors. To obtain the result, report is generated for the cell and total temperatures, surface report is generated for the cell, PCM as well as interfaces also. The time step is taken as 1 with 100 s flow time and 20 iterations.

2.3. Inertial Boundary Condition

The whole system and the coolant inlet were initially at 300 K. The coolant boundary at the inlet was defined as a velocity-inlet with a speed of 0.1 m/s, while the coolant exit was modeled as a pressure-outlet at 0 Pa (atmospheric pressure). Natural convection to the surroundings was included by taking the temperature of the ambient as 300 K and a convective heat transfer coefficient of 5 W/m^2K to all external surfaces of the BTMS and the Li-ion cells. Both the exterior surface of the enclosure and the interior surface of the cooling plate were treated as no-slip walls.

3. Results and Discussion

3.1. Mesh Generation

Fig. 4 presents the finite element discretization of an 18650-format cylindrical lithium-ion battery module, including its structural casing and auxiliary components, as modeled in ANSYS 2024 R1. The meshing process was carried out using a uniform element size of 0.0012 m to ensure a high-resolution geometric representation while maintaining computational efficiency.

Fig. 4 displays the complete battery module with the protective casing housing the cylindrical cells. The cells are rendered in distinct colors to visually distinguish individual units and facilitate mesh verification. The structured hexahedral mesh ensures consistent element distribution across the assembly, minimizing numerical errors during solution.

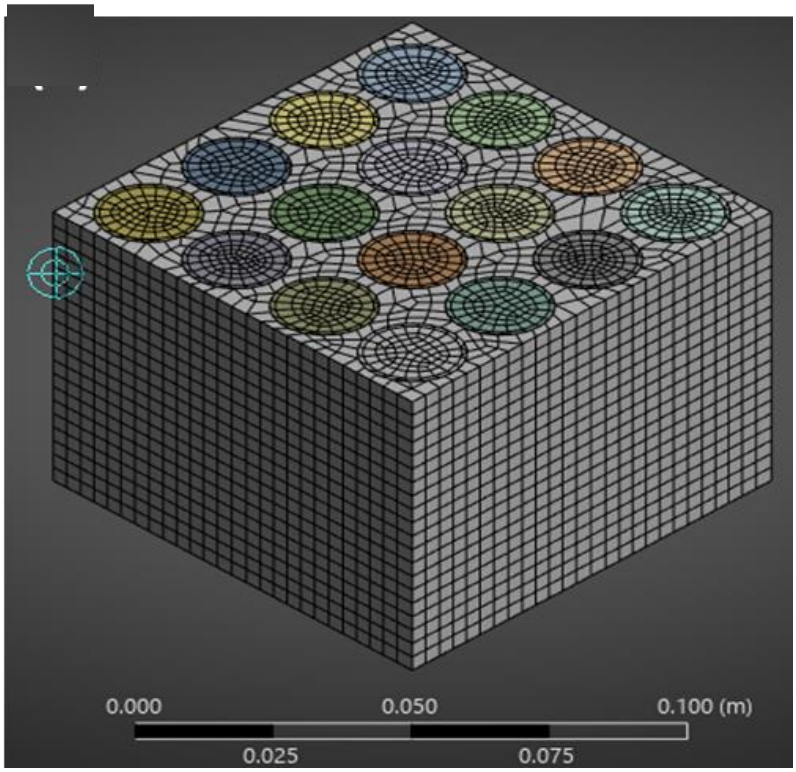

Fig. 4. Mesh generated diagram for the battery assembly

3.2. Temperature variation analysis

The **Fig. 5 (a)** presents the steady-state thermal response of an 18650-format lithium-ion battery module subjected to forced air cooling at an inlet velocity of 0.1 m/s. The airflow direction and outlet configuration are indicated in (a), with arrows representing velocity vectors along the designated inlet and outlet planes. The simulation was conducted using a coupled electro-thermal

model, where the heat generation rate within each cell was determined as a function of the applied C-rate.

Fig. 5 (b) corresponds to a discharge rate of 1C, where the peak surface temperature reaches approximately 300.21 K. The temperature field is nearly uniform, indicating minimal thermal gradients between cells. This is attributed to the low internal heat generation rate at 1C, which allows convective cooling to maintain temperature homogeneity. The maximum cell surface temperature increases to approximately 301.83 K, with a more pronounced temperature rise at the central cells (Fig. 5 (c)). The reduced exposure of these inner cells to the cooling airflow results in a mild thermal gradient, with outer cells exhibiting slightly lower temperatures due to direct convective contact. Fig. 5 (d) illustrates the 5C discharge case, where the maximum recorded surface temperature rises sharply to approximately 304.46 K. At this high C-rate, the internal heat generation significantly outweighs the cooling capacity of the 0.1 m/s airflow, leading to steeper radial temperature gradients. The central cells act as thermal hotspots, while edge cells remain relatively cooler due to enhanced heat dissipation to the surroundings.

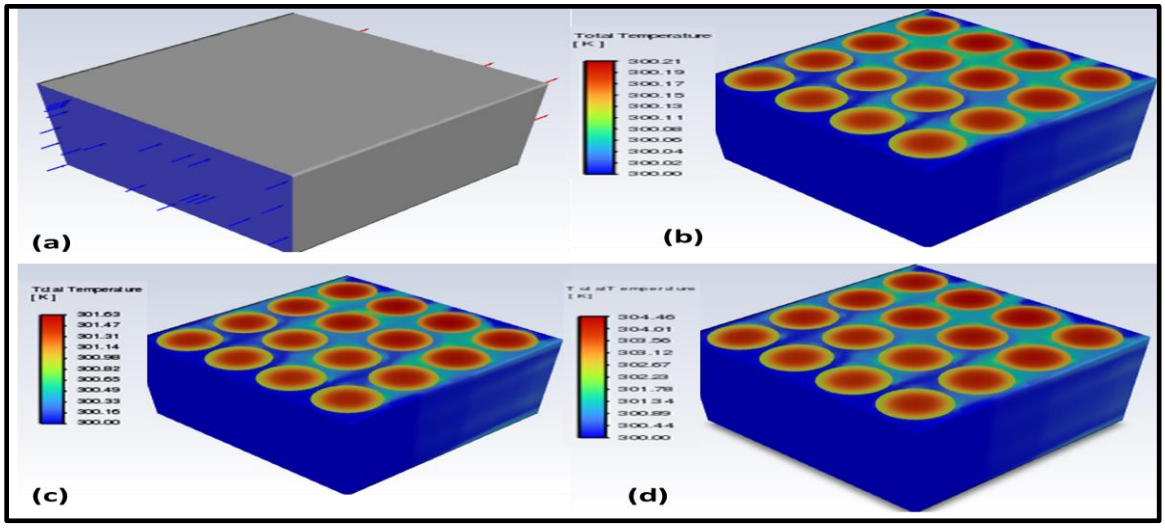

Fig. 5. *Contour of the battery module showing the variation of temperature with different c rates. (a) shows the inlet and outlet of the module, while (b), (c), and (d) are the contour of surface variation for 1C, 3C and 5C rates*

Change in surface temperature

Maximum and minimum surface temperatures were read from the steady-state thermal solution contour plots (color bars) produced in ANSYS 2024 R1. The inlet air temperature was set to 300.00 K; therefore $\Delta T_{max} = T_{max} - 300.00$ K and it is reported in the **Table 2** for all three cases of the C-rates. Thermal gradient reported here is the global difference between maximum and minimum surface temperatures from the same solution field. Hotspot locations were identified visually from the contour plots and correspond to centrally located cells with reduced exposure to convective cooling.

Table 2. *Maximum surface and cell temperatures and observation found from the contour of the battery module.*

C-Rate	Maximum Surface Temperature (K)	Temperature Rise (K)	Observation
1C	300.21	0.21	Nearly uniform temperature; no distinct hotspots.
3C	301.83	1.83	Small hotspots at central cells; outer cells cooler due to direct airflow.

5C	304.46	4.46	Pronounced hotspots in central region; larger radial gradients.

Total temperature of the battery module observed from the graph deduced by the ANSYS software is represented in the **Fig. 6.** Total temperature is the average of the temperatures of the battery module. From the figure, it can be observed that trend of total temperature is similar to the cell temperature. Total temperature does not vary significantly for the 1C, while it is higher for the 3C and 5C rate. The total temperature as compared to the maximum cell temperature is about 50%, 27% and 15% lower. It indicates that heat transfer rate is insignificant and can be improved by increasing the speed of the air or by changing the types of the flow medium. This is how, the effect of C rate on the cell temperature and total; temperature has been optimized and it was found that 5C rate is a concern and should be minimized the cell temperature by opting the active BTMs or passive BTMS. However, active BTMS reduce the efficiency of the battery because of the power consumption in the circulation of flowing media in the battery module.

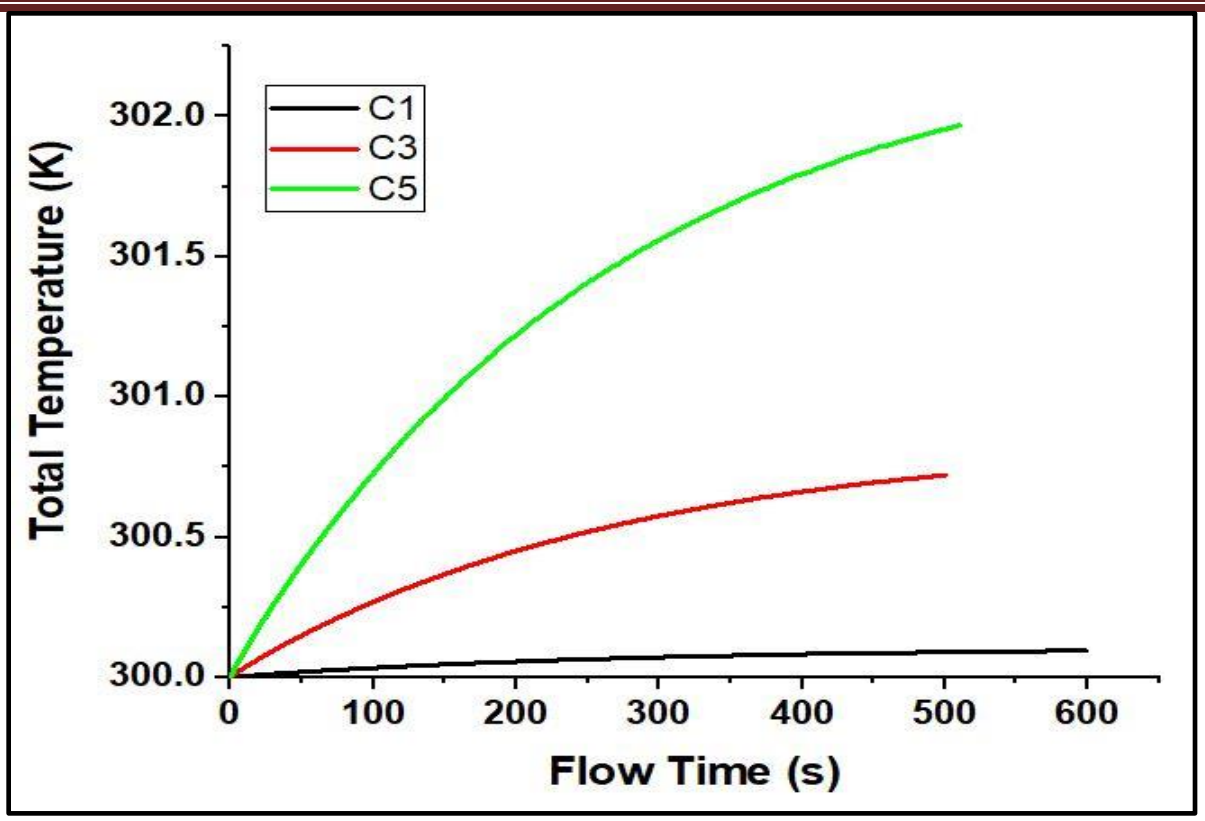

Fig. 6. *Variation of total temperature in the battery module with flow time for the 1C, 3C and 5C rates*

4. Conclusions

On the basis of above results and discussion, flowing conclusions can be made-

- The simulation confirms that cell temperature increases with higher C-rates, with maximum surface temperatures rising from 300.21 K at 1C to 304.46 K at 5C. Temperature distribution remains uniform at 1C, indicating effective natural heat dissipation under low discharge conditions.
- At 3C discharge, small hotspots appear in the central cells, while outer cells remain cooler due to direct airflow exposure. While at 5C discharge, the module exhibits

pronounced hotspots and steep radial gradients, posing risks of reduced efficiency and potential thermal runaway.

- The total average module temperature follows a similar trend to cell surface temperature, showing significant increase at higher C-rates. This study emphasizes that thermal management design must be aligned with operating C-rates to ensure safety, extend battery life, and maintain vehicle performance.

References

[1] M. Alda, "Transportation Emissions Worldwide-Statistics & Facts," ed, 2024.

[2] M. Varma, H. Mal, R. Pahurkar, and R. Swain, "Comparative analysis of green house gases emission in conventional vehicles and electric vehicles," *International Journal of Advanced Science and Technology,* vol. 29, pp. 689-695, 2020.

[3] A. Masakure, A. Gill, and M. Singh, "The Impact of Battery Charging and Discharging Current Limits on EV Battery Degradation and Safety," in *2023 3rd Asian Conference on Innovation in Technology (ASIANCON)*, 2023, pp. 1-5.

[4] J. Xie and Y. C. Lu, "Designing nonflammable liquid electrolytes for safe Li-ion batteries," *Advanced materials,* vol. 37, p. 2312451, 2025.

[5] G. Kalita, R. Otsuka, T. Endo, and S. Furukawa, "Recent advances in substitutional doping of AB5 and AB2 type hydrogen storage metal alloys for Ni-MH battery applications," *Journal of Alloys and Compounds,* p. 179352, 2025.

[6] F. Pang, X. Chen, X. Li, B. Wang, Y. Wu, Y. Xiao, X. Qu, X. Liu, S. Gao, and D. Wang, "Corrosion resistance of PbSrSnAl positive grid alloys for lead-acid batteries," *Electrochimica Acta,* vol. 519, p. 145835, 2025.

[7] R. K. Daniels, V. Kumar, and A. Prabhakar, "A comparative study of data-driven thermal fault prediction using machine learning algorithms in air-cooled cylindrical Li-ion battery modules," *Renewable and Sustainable Energy Reviews,* vol. 207, p. 114925, 2025.

[8] S. D. Gelam, S. Maddipatla, C. Chicone, and M. Pecht, "Anisotropic expansion-induced stress analysis of cylindrical Li-ion batteries," *Journal of Power Sources,* vol. 656, p. 238104, 2025.

[9] Q. Li, R. Song, and Y. Wei, "A review of state-of-health estimation for lithium-ion battery packs," *Journal of Energy Storage,* vol. 118, p. 116078, 2025.

[10] M. Murugan, P. Elumalai, K. Vijayakumar, M. Babu, K. Suresh Kumar, M. Ganesh, L. Kuang, and S. Prabhakar, "A Comprehensive Review of Thermal Management Methods and Ideal System Design for Improved Electric Vehicle Battery Pack Performance and Safety," *Energy Science & Engineering,* vol. 13, pp. 1011-1036, 2025.

[11] X. Liu, "Battery management system of electric vehicles," Nanyang Technological University, 2025.

[12] C. Wang, Z. Chen, Y. Shen, and J. Li, "Simulation analysis of battery thermal management system for electric vehicles based on direct cooling cycle optimization," *Applied Thermal Engineering,* vol. 268, p. 125938, 2025.

[13] Y. Zhao, Z. He, W. Liu, L. Chen, H. Pu, Y. Jiang, S. Li, and X. Cai, "Vibration-assisted active and passive collaborative cooling thermal management system: Performance study of thermoelectric cooling and phase change materials to enhance thermal stability of lithium-ion batteries," *Journal of Energy Storage,* vol. 117, p. 116256, 2025.

[14] J. Yu, X. Sun, X. Shen, D. Zhang, Z. Xie, N. Guo, and Y. Wang, "Stack pressure-A critical strategy and challenge in performance optimization of solid state batteries," *Energy Storage Materials,* vol. 76, p. 104134, 2025.

[15] A. Zain, D. Suranto, A. Budiprasojo, C. Karimah, F. Azhar, and M. Haryanto, "Applications of 18650 lithium-ion batteries pack in 3 kw electric vehicles," in *IOP Conference Series: Earth and Environmental Science*, 2025, p. 012056.

[16] A. Lemmassi, A. Derouich, A. Hanafi, M. Benmessaoud, and N. El Ouanjli, "Design and conception of an electrical power system for 1U CubeSat using MATLAB/Simulink," *The European Physical Journal Plus,* vol. 140, p. 45, 2025.